PHYSICAL REVIEW E **84**, 041808 (2011)

Glass transition dynamics of stacked thin polymer films

Koji Fukao,[*] Takehide Terasawa, Yuto Oda, Kenji Nakamura, and Daisuke Tahara
Department of Physics, Ritsumeikan University, Noji-Higashi 1-1-1, Kusatsu 525-8577, Japan

(Received 6 September 2011; published 24 October 2011)

The glass transition dynamics of stacked thin films of polystyrene and poly(2-chlorostyrene) were investigated using differential scanning calorimetry and dielectric relaxation spectroscopy. The glass transition temperature T_g of as-stacked thin polystyrene films has a strong depression from that of the bulk samples. However, after annealing at high temperatures above T_g, the stacked thin films exhibit glass transition at a temperature almost equal to the T_g of the bulk system. The α-process dynamics of stacked thin films of poly(2-chlorostyrene) show a time evolution from single-thin-film-like dynamics to bulk-like dynamics during the isothermal annealing process. The relaxation rate of the α process becomes smaller with increase in the annealing time. The time scale for the evolution of the α dynamics during the annealing process is very long compared with that for the reptation dynamics. At the same time, the temperature dependence of the relaxation time for the α process changes from Arrhenius-like to Vogel-Fulcher-Tammann dependence with increase of the annealing time. The fragility index increases and the distribution of the α-relaxation times becomes smaller with increase in the annealing time for isothermal annealing. The observed change in the α process is discussed with respect to the interfacial interaction between the thin layers of stacked thin polymer films.

DOI: 10.1103/PhysRevE.84.041808 PACS number(s): 61.41.+e, 71.55.Jv, 81.05.Lg, 77.22.Ch

I. INTRODUCTION

It is well known that amorphous materials exhibit structural and dynamical changes at the glass transition temperature T_g. As temperature decreases, the relaxation time of the α process, which is the segmental motion of polymers, becomes longer and at T_g it reaches a macroscopic time scale such as 10^2–10^3 sec. As a result, below T_g there is almost no mobility of the material due to the α process and the system can be regarded as a glassy state [1]. Recent investigations have revealed that the T_g of thin polymer films or small molecules in a confined geometry decreases with decreasing film thickness or size of nanopores in many cases, although there are some contradictory results [2–21]. Physical origins for the depression of the T_g include such candidates as surface or interfacial effects [22], and confinement effects in thin-film geometry [23].

Recently, the glass transitions of stacked thin films have been investigated using differential scanning calorimetry (DSC) [24,25]. The glass transition temperature T_g of stacked thin polymer films is dependent on the thickness of the single layers of the stacked thin films, which is similar to that for single thin polymer films. Furthermore, T_g is increased by annealing above T_g and approaches that of the bulk system, which suggests that stacked thin films prepared by an appropriate method can maintain the thin-film properties of the glass transition dynamics.

We have previously reported an investigation on the glass transition behavior of single thin films and stacked thin films of poly(2-chlorostyrene) (P2CS) by capacitance measurements as a means to determine the thickness dependence of the glass transition dynamics in single and stacked P2CS thin films [26]. The following results were obtained: (1) The T_g of single P2CS thin films was found to decrease with decreasing film thickness in a similar way to that observed for polystyrene (PS) thin films [2,11,12]. The magnitude of the depression ΔT_g of T_g for the stacked thin films from that for the bulk samples was larger than that for single thin films supported on a substrate with a thickness of 12–18 nm. Here, the stacked thin films consist of 10 layers of 12 nm thick single thin films. (2) Annealing could result in a decrease of ΔT_g for the stacked thin films.

The difference between the stacked thin films and the single films is the existence of interfaces between the thin layers. Therefore, from the previously observed results it can be expected that the interfacial interaction between thin polymer layers could play a crucial role in determining the depression of T_g for thin polymer films [27,28]. However, a detailed mechanism for the depression of T_g in the presence of interfaces is still unclear. According to our previous results, how the interface disappears for annealing above T_g and how the change in the interfacial interaction affects the T_g of stacked thin films must be determined for the purpose of elucidating the T_g depression mechanism for stacked thin polymer films.

In this investigation, we measured the thermal and dielectric quantities of stacked thin films using DSC and dielectric relaxation measurements for the isothermal annealing process above T_g, to identify the change in the glass transition dynamics in stacked thin polymer films.

The experimental details are given in Sec. II. The thermal properties of glass transitions for stacked thin PS films as observed by DSC are given in Sec. III, and the evolution of glass transition dynamics for stacked thin films of P2CS as observed by dielectric measurements is given in Sec. IV. Furthermore, the change in dielectric loss spectra is discussed in Sec. V, and concluding remarks are given in Sec. VI.

II. EXPERIMENT

P2CS and PS used in this study were purchased from Polymer Source, Inc., and General Science Co., Ltd., respectively. The weight-averaged molecular weight (M_w) and the molecular weight distribution (M_w/M_n, where M_n is the

---

[*] fukao.koji@gmail.com

TABLE I. Thickness of a single layer d, total weight, number of stacked layers, and T_g (K) measured by DSC for stacked PS thin films prepared for the DSC measurements.

d (nm)	Weight (mg)	No. of layers	T_g (K)
70	0.623	73	369
55	0.528	100	364
40	0.611	130	361
20	0.786	224	353
13	0.899	400	350
Bulk	1.361	1	376

number-averaged molecular weight) were $M_w = 3.3 \times 10^5$ and $M_w/M_n = 2.2$ for P2CS, and $M_w = 2.8 \times 10^5$ for PS. The structure of P2CS is similar to that of PS, except for the presence of a chlorine atom on the benzene ring. However, the polarity of P2CS is much larger than that of PS; therefore, P2CS can be regarded as an ideal system for the dielectric measurements.

Stacked thin films were prepared in the following way [26]. Single ultrathin films of various thickness were prepared on glass substrates by spin coating of a toluene solution. The thickness was controlled by changing the solution concentration and was evaluated directly by atomic force microscopy measurements [11]. The film was floated onto the surface of water and transferred to the top of a substrate or a stack of polymer thin films on a substrate. This procedure, using ultrathin films with the same thickness, was repeated until the total number of stacked thin layers reached several hundred for the DSC measurements and 10 layers for the dielectric measurements, as listed in Tables I and II. For the dielectric measurements, the first layer of P2CS was prepared directly onto an Al-deposited glass substrate and subsequent thin layers were prepared according to the above procedure. For the DSC measurements, a Teflon plate was used as a substrate. The stack of thin films, which consisted of several hundred thin layers, was detached from the Teflon substrate using a razor blade.

A commercial instrument (TA Instruments, Q200) was used for the DSC measurements. DSC measurements were first conducted for the heating process from 303 to 403 K at a rate of 10 K/min, and then for the cooling process down to 303 K at the same rate. DSC measurements were repeated three times to confirm reproducibility. The stacked samples used for the DSC measurements were then annealed at 523 K for 12 h *in vacuo*. DSC measurements were performed for the heating and cooling processes between 403 and 303 K. Nitrogen gas was flowed at 30 mL/min during the DSC measurements.

TABLE II. Thickness of a single layer d, number of stacked layers, isothermal annealing temperature T_a, and T_g (single thin film with a thickness of d) for stacked P2CS thin films prepared for the dielectric relaxation measurements. Asterisk (*) indicates that the value of T_g is evaluated for a single thin film with thickness d, rather than the total stack thickness, from an approximation given in Ref. [26].

d (nm)	No. of layers	T_a (K)	T_g (K)*
18.5	10	425	381.0
15.4	10	416	380.1
10.0	10	412	378.6
9.6	10	422	378.5

An LCR meter (Agilent Technology, 4284A) was used for the dielectric measurements. One measurement for the frequency f range from 20 Hz to 1 MHz took approximately 50 s. Prior to the dielectric measurements, several heating and cooling processes through T_g were conducted for stabilization of the measurements. Following that, the dielectric measurements were performed repeatedly for the following temperature cycles. One temperature cycle consists of two successive parts:

(1) Cooling and heating processes between 433 and 273 K at a rate of 1 K/min were conducted *twice*.

(2) After the ramping process, the temperature was changed from 433 K to T_a (=412 $\sim$ 425 K) and was then kept at T_a for 10 h (isothermal annealing at T_a).

These measurements showed that the two dielectric loss spectra observed successively in the temperature domain at a given frequency in part (1) agree with each other; therefore, the annealing effect for the ramping process (1) between 273 K and 433 K was determined to be negligible compared with that for the isothermal annealing process. The annealing time t_a can be well defined by the total time for which the films remain at the annealing temperature T_a. Hence, t_a for the nth isothermal annealing cycle starts from $10(n-1)$ h.

III. THERMAL PROPERTIES DETERMINED BY DIFFERENTIAL SCANNING CALORIMETRY

Figure 1 shows the temperature dependence of the total heat flow during the heating process at a rate of 10 K/min for stacked PS thin films with various single-layer thicknesses, as listed in Table I. Figure 1(a) shows an anomaly in the total heat flow around 350–380 K, which is associated with the glass transition of PS, and the temperature at which the anomaly occurs can be regarded as T_g. Values of T_g, evaluated as the middle temperature of the anomalous region, are listed in Table I. The T_g for stacked PS films increases from 350 to 369 K with increasing single-layer-film thickness in the stacked thin films, even if the total thickness of the stacked thin polymer films is sufficiently large to nullify the dependence of T_g on the thickness. The magnitude of the T_g depression for the stacked thin films from that for the bulk is slightly larger than that for the single thin polymer film supported on a substrate [2,11]. In contrast, the depression for the stacked thin films is smaller than that for the freely standing thin films [29]. This result for the T_g of stacked thin films is consistent with that reported in the literature [24,25].

Figure 1(b) shows the temperature dependence of the total heat flow observed after annealing at 523 K for 12 h *in vacuo*. The anomalous region, i.e., T_g, is located almost at the same position, regardless of the single-layer thickness. The observed value of T_g is approximately 376 K, which is almost equal to that for the bulk sample. This result suggests that T_g of the stacked thin films increases and approaches the bulk T_g after annealing at 523 K *in vacuo*. In other words, the bulk-like glass transition dynamics could be restored after annealing at high temperature for 12 h.

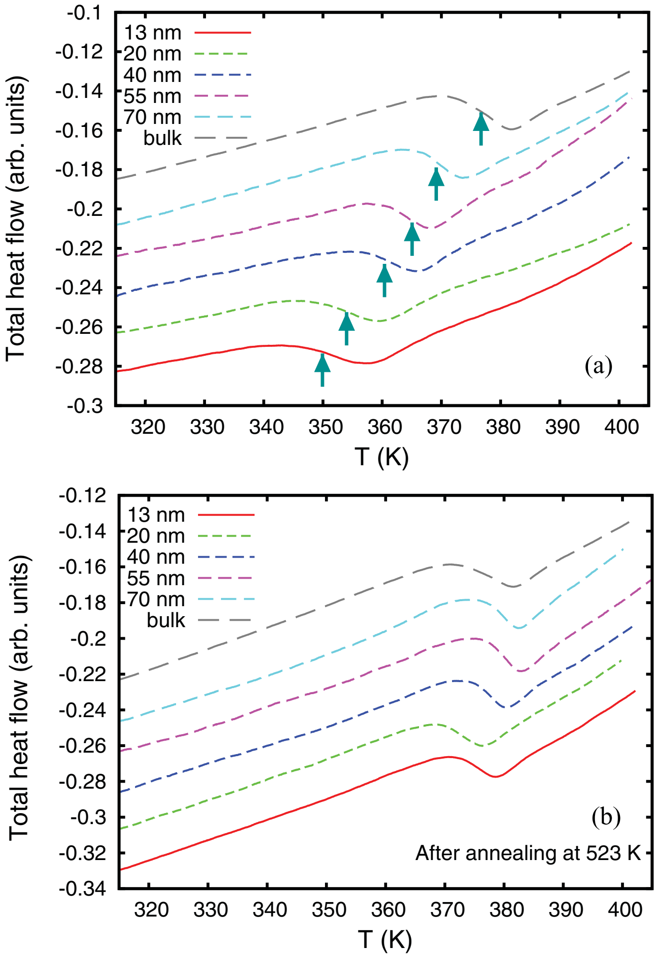

FIG. 1. (Color online) Temperature dependence of the total heat flow for stacked PS thin films with various single-layer thicknesses, from 13 nm to that of the bulk value, during the heating process at a rate of 10 K/min. (a) As-stacked thin PS films, and (b) after annealing at 523 K for 12 h. Each curve is shifted slightly along the vertical axis for ease of comparison.

Annealing at high temperature diminishes the contrast at the interface between two thin layers, which suggests the possibility that the glass transition temperature could be controlled through interfacial interaction.

IV. EVOLUTION OF GLASS TRANSITION DYNAMICS FOR STACKED THIN FILMS

To demonstrate the effect of annealing on the glass transition dynamics of stacked P2CS thin films in more detail, *in situ* dielectric measurements were performed during successive isothermal annealing processes at a given annealing temperature, T_a. For these measurements several stacked thin films of P2CS were prepared, as listed in Table II. The thickness of each single layer was between 9 and 18 nm, and the number of stacked layers for each sample for the dielectric measurements was 10. The annealing temperature ranged between 412 and 425 K.

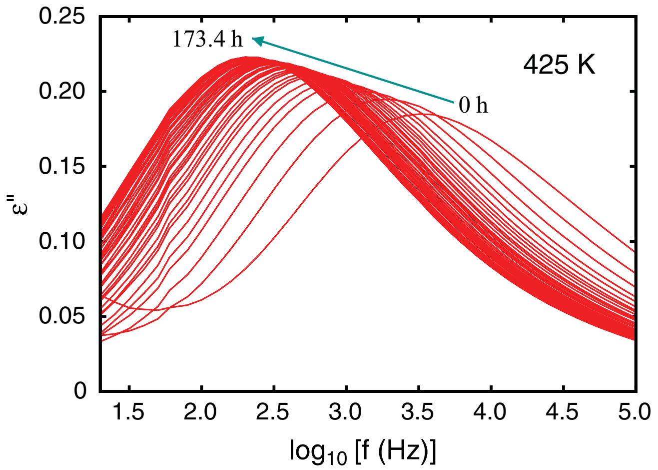

FIG. 2. (Color online) Evolution of ε'' spectra as a function of annealing time t_a for the successive isothermal annealing of stacked P2CS thin films at 425 K. The thickness of each thin layer was 18 nm. The annealing times t_a were 0, 3.4, 6.8, 10, 13.4, 16.8, 20, . . . , 173.4 h.

A. Shift in the dielectric-loss peak due to the α process

Figure 2 shows the evolution of the dielectric loss spectra in the frequency domain observed for the successive isothermal annealing process of stacked P2CS thin films of 18 nm thick layers. The dielectric loss ε'' vs frequency f is plotted for various times $t_a = 0 \sim 173.4$ h of isothermal annealing at 425 K. The dielectric loss peak due to the α process is located around $10^{3.6}$ Hz at $t_a = 0$ h. The frequency at which the dielectric loss has a peak due to the α process is denoted by f_α. The location of the peak f_α decreases down to $10^{2.3}$ Hz and the peak height increases with increasing annealing time, which suggests a slowing of the α-process dynamics with increase in the annealing time.

As described in Sec. II, two dielectric measurements in the temperature domain were conducted between two successive isothermal annealing processes for 10 h. The results suggest that there is no appreciable annealing effect of the ramping process between the repeated isothermal annealing processes for 10 h. The value of f_α for the isothermal annealing process was evaluated as a function of the annealing time t_a from the data presented in Fig. 2. Figure 3 shows the time evolution of f_α thus obtained for four different stacked thin films with various thickness and annealing temperatures.

Figure 3 shows that at the beginning of isothermal annealing, the frequencies $\log_{10} f_\alpha$ are located at 3.5, 3.3, 2.9, and 2.2 for $T_a = 425, 422, 416$, and 412 K, respectively. At a given T_a, the value of f_α for stacked thin films is higher than that observed for a single thin film with a thickness equal to that of a single layer in the stacked thin films. However, as the annealing time increases at a given T_a, the value of $\log_{10} f_\alpha$ decreases monotonically down to 2.4, 1.9, 1.4, and 0.75 for $T_a = 425, 422, 416$, and 412 K, respectively. The final values almost correspond to those observed for single thin films with thicknesses almost equivalent to the total thickness of the stacked thin films. (See the solid curve for single thin films with a thickness of 120 nm in Fig. 9.) This result suggests that the α dynamics of the stacked thin films approach those of

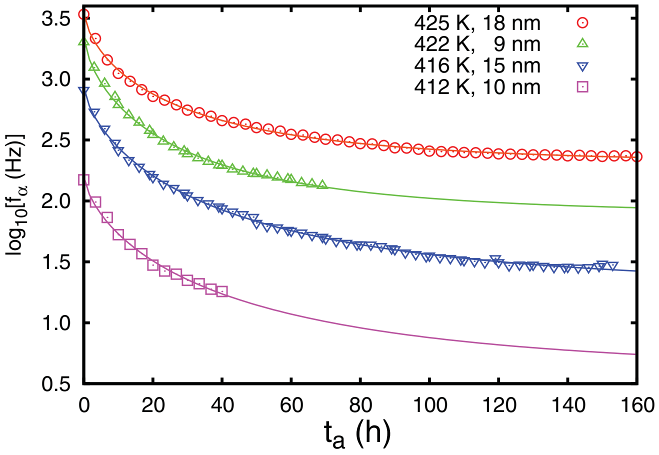

FIG. 3. (Color online) Dependence of f_α on the annealing time t_a for successive isothermal annealing process at $T_a = 425$, 422, 416, and 412 K for stacked P2CS thin films, where the thickness of a single layer was 9–18 nm. The solid curves were calculated using Eq. (1)

thicker films with thicknesses larger than 100 nm from those of a single ultra thin film.

Figure 4 shows the dependence of T_g on the annealing time. The T_g values were determined in the temperature domain for the ramping process from measurements obtained between two successive isothermal annealing processes at $T_a = 425$ K for stacked thin films of 18 nm thick P2CS layers. As shown in Refs. [11,12], the temperature coefficient of the real part of electric capacitance C' observed for high frequency (i.e., 100 kHz) changes significantly through the glass transition temperature, because the thermal expansion coefficient of the glassy state is much smaller than that of the liquid state. On the basis of this phenomenon, T_g is determined from the crossover temperature of C' observed during the ramping process at a constant rate. Figure 4 shows that the T_g of the stacked thin films increases with increase in the annealing time. When taking the value of T_g for the heating process in Fig. 4, the T_g at $t_a = 0$ of the stacked thin films is much smaller than that for a single thin film with similar thickness ($T_g = 380.8$ K for $d = 18$ nm [26]), while T_g at $t_a = 180$ h is almost equivalent to that for the bulk ($T_g = 387.8$ K for $d = 180$ nm [26]). Although there is a slight difference in T_g between the heating and cooling processes, as usually observed in other T_g measurements, the dependence of f_α on the annealing time for isothermal annealing is qualitatively consistent with the change in T_g.

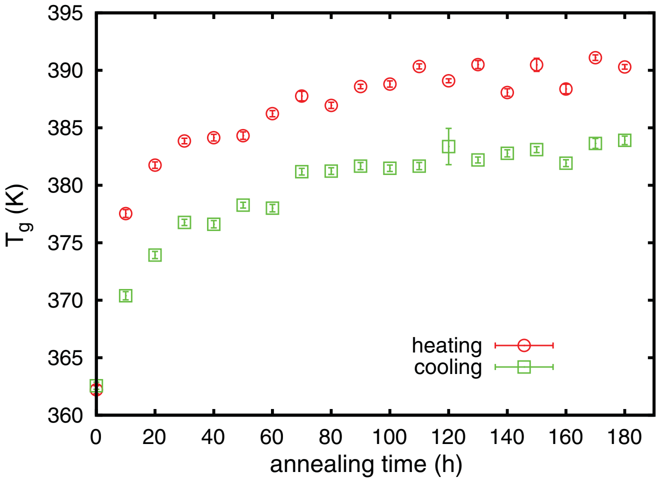

FIG. 4. (Color online) Dependence of T_g on the annealing time t_a observed for the ramping process in the temperature domain between two successive isothermal annealing processes for stacked thin films of 18 nm thick P2CS layers.

The time evolution of f_α and T_g in Figs. 3 and 4 suggests that there should be a change in the dynamics of the stacked thin films with a characteristic time scale of several tens of hours for isothermal annealing.

B. Time evolution of f_α

A slow change in f_α and T_g was observed during isothermal annealing of the stacked P2CS thin films. Here, we will investigate the dependence of $f_\alpha(t_a)$ on the annealing temperature and possibly on the thickness of the single layers of the stacked thin films. Figure 3 shows that the annealing-time dependence of f_α observed during the isothermal annealing process can well be reproduced using the following equation:

$$\log_{10} f_\alpha(t_a) = \log_{10} f_\alpha^\infty + \left(\log_{10} f_\alpha^0 - \log_{10} f_\alpha^\infty\right) \exp[-(t_a/\tau)^n], \quad (1)$$

where f_α^0 and f_α^∞ are the values of f_α at $t_a = 0$ and ∞, τ is the characteristic time, and n is the exponent of the stretched exponential function. The solid curves given in Fig. 3 are calculated using Eq. (1). The best fitting parameters are given in Table III.

According to Eq. (1), the following scaling function can be obtained:

$$\mathcal{F}_\alpha(\tilde{t}_a) = \exp\left(-\tilde{t}_a^n\right), \quad (2)$$

where

$$\mathcal{F}_\alpha(\tilde{t}_a) \equiv \log_{10}\left(\frac{f_\alpha}{f_\alpha^\infty}\right) \Big/ \log_{10}\left(\frac{f_\alpha^0}{f_\alpha^\infty}\right), \quad (3)$$

$$\tilde{t}_a \equiv \frac{t_a}{\tau}. \quad (4)$$

In Fig. 5, all $f_\alpha(t_a)$ data are plotted after scaling via $\mathcal{F}_\alpha(\tilde{t}_a)$ using Eqs. (3) and (4). Figure 5 shows that the time evolution of the α-peak frequency f_α can well be reduced to a single master curve for various values of T_a (and d). Therefore, we can expect that the observed time dependence of f_α can be controlled by a common mechanism, regardless of T_a and d. Furthermore, the exponent of Eq. (1) is given by the following relation: $n =$

TABLE III. Values of f_α^∞, f_α^0, τ obtained by fitting the observed data using Eq. (1) for various annealing temperatures T_a, and the thickness of a single layer, d. Here, the exponent n is fixed at 0.70.

T_a (K)	d (nm)	$\log_{10} f_\alpha^\infty$	$\log_{10}(f_\alpha^0/f_\alpha^\infty)$	τ (h)
425	18.5	2.31 ± 0.01	1.22 ± 0.01	28.9 ± 0.7
422	9.6	1.90 ± 0.03	1.45 ± 0.02	28.0 ± 1.7
416	15.4	1.29 ± 0.01	1.65 ± 0.01	43.0 ± 1.2
412	10.0	0.6 ± 0.18	1.60 ± 0.17	45 ± 11

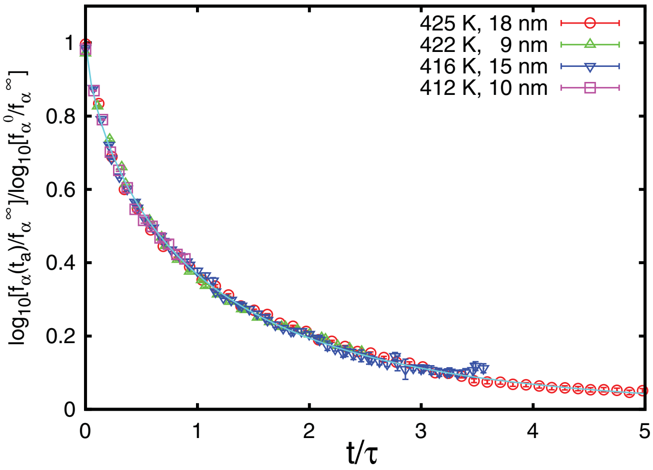

FIG. 5. (Color online) $F_\alpha(\tilde{t_\alpha})$ vs $\tilde{t}_a$ for stacked P2CS thin films for various values of T_a and d. The solid curve is calculated using Eq. (2) with $n = 0.70 \pm 0.03$.

0.70 ± 0.03. Therefore, a single exponential function could be a good approximation for this slow-changing process.

Figure 6 shows the characteristic time τ for the change in the α-peak frequency f_α for this process observed during isothermal annealing at T_a. The characteristic time τ increases with decreasing annealing temperature. It should be noted that there is an ambiguity in determining the temperature dependence of τ, due to the small number of observed points. Nevertheless, if we assume that the temperature dependence of τ is given by $\tau(T_a) = \tau_0 \exp(U/T_a)$ (where τ_0 and U are the constants), then a straight line can be obtained in Fig. 6 with the parameter $U = 6.2 \pm 1.9$ kcal/mol. This activation energy is much smaller than of the common value for the β process of polystyrene ($U \sim 35$ kcal/mol) [30].

C. Diffusion of polymer chains

A change in the contrast at the interface between two neighboring layers is expected to occur during the isothermal annealing process. With increasing annealing time, the contrast decreases and, as a result, the morphology of the stacked thin film approaches that of the bulk film. It is clear that the diffusion of polymer chains is promoted during isothermal annealing, and the polymer chain undergoes interdiffusion between neighboring layers [31]. However, there is a question here as to whether the presently observed change is due solely to chain diffusion.

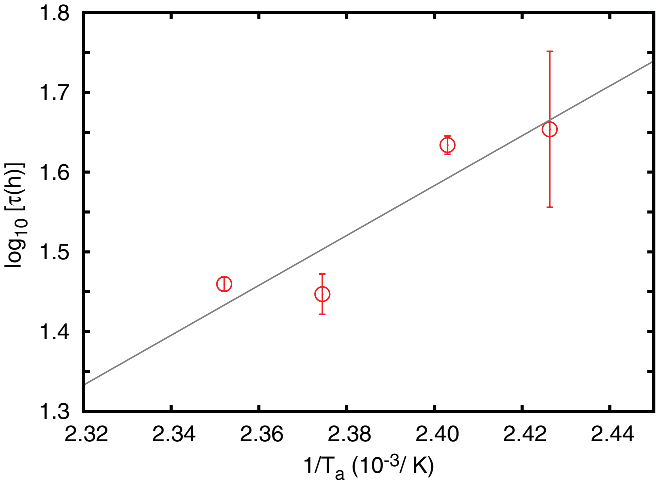

FIG. 6. (Color online) Arrhenius plot of τ as a function of T_a for stacked P2CS thin films with various values of T_a and single-layer thicknesses d ($9.6 \sim 18.5$ nm).

In order to answer this question, we estimate the chain diffusion during isothermal annealing. The temperature dependence of the diffusion constants measured using secondary ion mass spectroscopy was reported for PS by Whitlow and Wool [31]. From these measurements, we have estimated the diffusion length of P2CS for isothermal annealing at T_a, as shown in Table IV. The glass transition temperature for the bulk is $T_g = 388.5$ K for P2CS [26] and $T_g = 370.5$ K for PS [11], so that the difference of T_g is $\Delta T_g = 18.0$ K. Therefore, the temperature dependence of the self-diffusion constant of P2CS, $D_{\mathrm{P2CS}}(T)$, was evaluated from that of PS, $D_{\mathrm{PS}}(T)$, reported in Ref. [31] using the relation $D_{\mathrm{P2CS}}(T) = D_{\mathrm{PS}}(T - 18.0\ \mathrm{K})$. The values D_{P2CS} for isothermal annealing at $T_a = 425$ and 412 K are given in Table IV. From D_{P2CS}, the diffusion length ℓ_{diff} was also evaluated for 10 h annealing at T_a. Table IV shows the diffusion length of P2CS is 57 nm for annealing at 425 K for 10 h. This length is much larger than the thickness of a single thin layer ($d = 18$ nm), even for isothermal annealing for 10 h. Therefore, it is expected that the polymer chains have already reached from one interface to the neighboring one, while the evolution of T_g and f_α still continues. However, this may be an unrealistic situation.

In order to avoid this contradictory situation, there could be two possible scenarios. First, in the above discussion, we adopted the diffusion constant from Ref. [31], which was evaluated from the diffusion constant of polymer chains at the interface between two bulk polymeric layers. Recent measurements have revealed the existence of heterogeneous dynamics in confined geometries, such as thin films and nanopores [32,33]. For stacked thin films of polymers, the dynamics vary with an essential dependence on the distance of the layer of interest from the free surface or from the substrate [34]. If such dynamical heterogeneity is taken into account, the diffusion of polymer chains could be restricted by the existence of an immobile region.

Second, the interface between the two polymer layers of as-stacked thin films may not be sufficiently smooth for good contact between the two layers. In this case, the diffusion of polymer chains between the two thin layers would be limited by improvement of the contact between the surfaces of the two thin layers. It has been reported that the area of indentation

TABLE IV. Diffusion constant D_{P2CS}, and diffusion length ℓ_{diff}, at two annealing temperatures for stacked P2CS thin films. D_{P2CS} is evaluated from that of PS reported in [31]. ℓ_{diff} is the diffusion length for isothermal annealing at T_a for 10 h.

T_a (K)	D_{P2CS} (cm^2/s)	ℓ_{diff} (nm)
425	9.0×10^{-16}	57
412	1.4×10^{-16}	22

increases approximately with the logarithm of time for the contact of two solid surfaces. This observation is related to the change in the quality of a contact [35,36]. As a result, the change in the interface between two thin layers could exhibit a very slow temporal change, as shown in the present measurements.

V. DYNAMICS OF THE α PROCESS FOR STACKED P2CS THIN FILMS

In this section, the time evolution of dielectric loss spectra for isothermal annealing process as a function of annealing time t_a is discussed to elucidate how the dynamics of the α process change with increase of the annealing time t_a.

A. Shape of the dielectric spectra

Figure 7 shows the frequency dependence of the dielectric loss normalized with respect to the peak position and height of the α process for 4 different annealing times during the isothermal annealing at $T_a = 425$ K for stacked thin films of 18 nm thick P2CS layers. The dielectric-loss data in the frequency domain at various temperatures and at a given annealing time $t_a = 10n$ (n is a positive integer) are extracted from the data measured for the heating process (1) between the $(n-1)$th and nth isothermal annealing processes. The normalized data show that the superposition with respect to the position of the α process does correspond well for the temperature range from 405 to 425 K, so that a master curve can be obtained.

As shown in Fig. 7, a master curve for the dielectric-loss spectra becomes narrower with increasing annealing time for the isothermal annealing process. For comparison, the dielectric-loss spectra of single thin P2CS films with thicknesses of 20, 120, and 1680 nm are given by dashed or dot-dashed curves in Figs. 7(a) and 7(d). This tendency in the stacked thin films is quite similar to that observed for the single thin P2CS films with increasing film thickness. Here, it should be noted that there is a slight deviation from the master curve at $t_a = 0$ h. The slight deviation is consistent with the existence of heterogeneity in the thin-film geometry [12,37].

Furthermore, in order to observe this narrowing of the dielectric spectra more quantitatively, the dielectric spectra

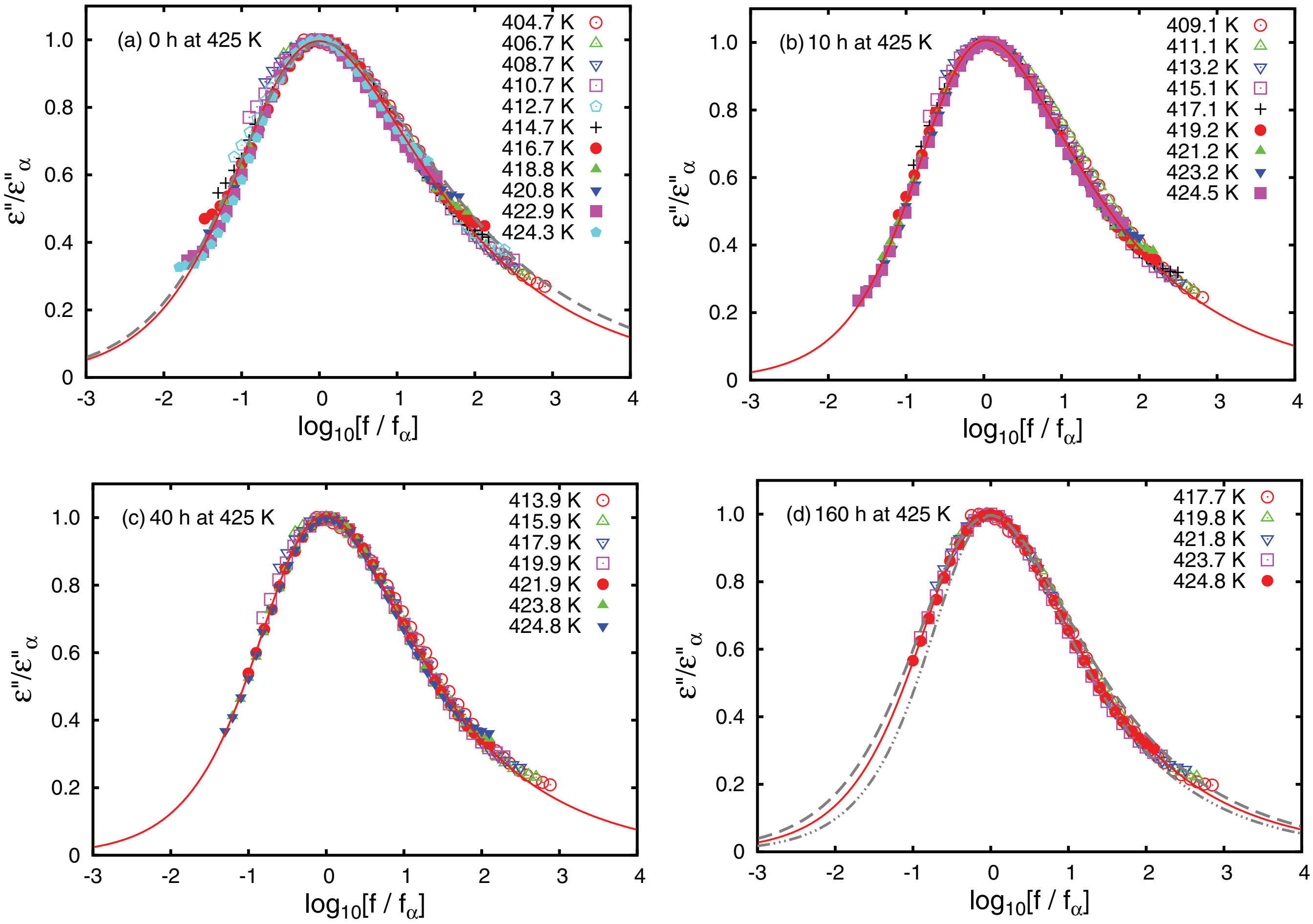

FIG. 7. (Color online) Time evolution of dielectric loss spectra normalized with respect to the position of the α process for isothermal annealing of stacked 18 nm thick P2CS thin films at $T_a = 425$ K. The annealing times are (a) 0, (b) 10, (c) 40, and (d) 160 h. The solid curves were obtained by fitting the normalized data for the stacked thin films to Eq. (5). The dashed curves in (a) and (d) were calculated from the fitting parameters for single thin films of P2CS with thicknesses of 20 and 120 nm, respectively. The dot-dashed curve in (d) is that for stacked thin films with a thickness of 1680 nm.

were fitted in terms of the Havriliak-Negami equation:

$$\varepsilon^*(\omega) = \frac{\Delta\varepsilon}{[1 + (i\omega\tau_0)^{1-\alpha_{HN}}]^{\beta_{HN}}}, \tag{5}$$

where $\omega = 2\pi f$, τ_0 is the relaxation time, $\Delta\varepsilon$ is the relaxation strength, and α_{HN} and β_{HN} are the shape parameters [38]. As shown by the solid curves in Fig. 7, Eq. (5) reproduces the observed master curves well at all annealing times.

Figure 8 shows the shape parameters, α_{HN} and β_{HN}, of Eq. (5) as a function of annealing time for stacked thin films of 18 nm thick P2CS layers. Both parameters increase with increasing annealing time for isothermal annealing at 425 K. Furthermore, using the α_{HN} and β_{HN} fitting parameters, the stretching parameter β_K of the Kohlrausch-Williams-Watts equation (KWW) can also be evaluated as a measure of the broadening of the relaxation time distribution [39]. Here, the β_K stretching parameter is given in the equation

$$\phi(t) = \exp[-(t/\tau_K)^{\beta_K}], \tag{6}$$

where $\phi(t)$ is the relaxation function, i.e., the relaxation function of the fluctuational correlation of dipole moments in the case of dielectric relaxation. There is an empirical relation among the α_{HN}, β_{HN}, and β_K parameters, as follows [40]:

$$\beta_K = [(1 - \alpha_{HN})\beta_{HN}]^{1/1.23}. \tag{7}$$

Using Eq. (7), the β_K stretching parameters can be evaluated and are found to increase with increase in the annealing time, as shown by the open square symbols in Fig. 8. In other words, the shape of the dielectric-loss spectra becomes sharper with increase in the isothermal annealing time.

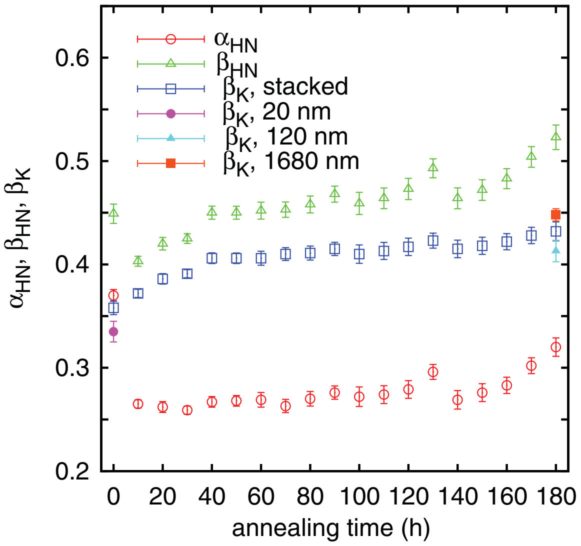

FIG. 8. (Color online) Annealing-time dependence of the shape parameters, α_{HN} and β_{HN}, from the HN equation, and the stretching exponent of the KWW equation β_K, for isothermal annealing at 425 K. The values of β_K are evaluated using Eq. (7). The corresponding values for single P2CS thin films with thicknesses of 20 (plotted at $t_a = 0$), 120, and 1680 nm (plotted at $t_a = 180$ h) are also presented for comparison.

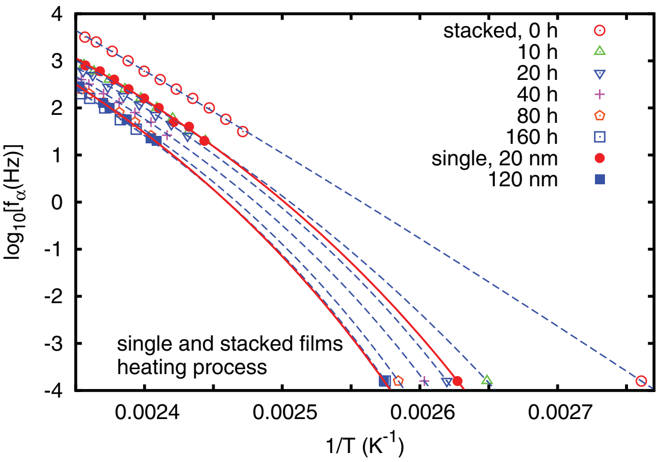

FIG. 9. (Color online) Dispersion map for the α process of both single thin films and stacked thin films of P2CS. For stacked thin films of 18 nm thick P2CS layers, the temperature dependence of f_α at various annealing times $t_a = 0$ to 160 h are plotted. The results for single thin films with thicknesses of 20 and 120 nm are also plotted.

B. Non-Arrhenius behavior of the α process

In order to interpret the present results both on T_g and f_α, a dispersion map of the α process was constructed for stacked thin films of 18 nm thick P2CS layers. Figure 9 shows the data observed for single thin P2CS films with thicknesses of 20 and 120 nm together with the results for stacked thin films. Here, the values of f_α are plotted for the temperature range of 400–425 K. Furthermore, the value of T_g for a given annealing time is also plotted as the point $(1/T_g, 1/2\pi\tau_g)$, where the characteristic time of the α process at T_g, τ_g, is assumed to be 10^3 s.

Comparison of the temperature and annealing time dependence of the relaxation times for the α process of stacked thin films of P2CS with those for single thin films of P2CS shows that the relaxation rate of the α process, f_α, becomes smaller with increasing annealing time for the stacked thin films, the relaxation rate for the stacked thin films at $t_a = 0$ is larger than that for a single thin film with a thickness of 20 nm, and f_α approaches that for the single thin film with a thickness of 120 nm with increasing annealing time. It is also noticed that for as-stacked thin films, the temperature dependence of the relaxation rate for the α process can be well described by an Arrhenius-type temperature dependence, while non-Arrhenius behavior becomes more pronounced with increasing annealing times. The curves are given using the Vogel-Fulcher-Tammann law:

$$f_\alpha = f_0 \exp[-U/(T - T_0)], \tag{8}$$

where f_0 is constant, U is an apparent activation energy (temperature), and T_0 is the Vogel temperature [41]. Figure 9 shows that Eq. (8) can reproduce the observed temperature dependence of the relaxation rate of the α process well for the isothermal annealing process. The Vogel temperature T_0 increases with increasing annealing time, in accordance with the increase in T_g for the isothermal annealing process of stacked thin films [26].

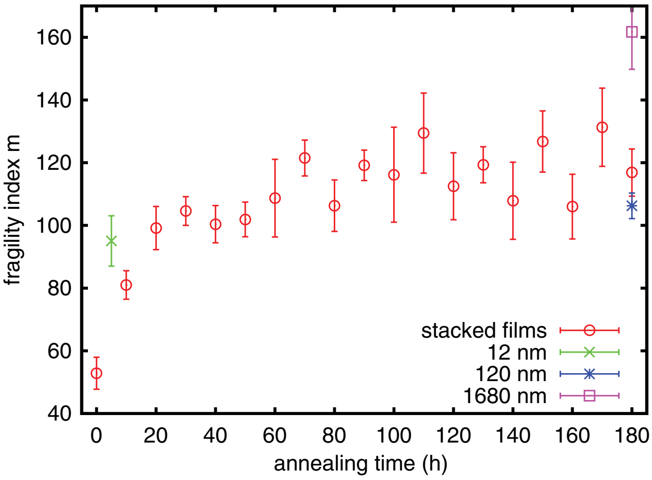

FIG. 10. (Color online) Dependence of the fragility index m on the annealing time for annealing at 425 K of stacked thin films of 18 nm thick P2CS layers. The fragility indices for single thin films with thicknesses of 12, 120, and 1680 nm are also plotted.

In order to evaluate the non-Arrhenius behavior in more detail, the fragility index m is evaluated according to the following equation for the temperature dependence of the α-relaxation times:

$$m = \left[\frac{d \log_{10} \tau_\alpha(T)}{d(T/T_g)}\right]_{T=T_g}, \qquad (9)$$

where $\tau_\alpha = 1/2\pi f_\alpha$ [42]. Figure 10 shows that the fragility index m increases with increase in the annealing time at $T_a = 425$ K. The glassy dynamics of the stacked thin films change from less fragile to more fragile for the isothermal annealing process. The interlayer interaction within the stacked thin films of P2CS may influence the fragility of polymeric systems, because the contrast at the interface is decreased with increasing annealing time.

On the base of the present measurements, we can say that both m and β_K increase with increasing annealing time for stacked thin films of P2CS. There should be a positive correlation between m and β_K, which is totally different from that observed for conventional glassy systems that have been reported in Refs. [43,44]. However, a similar positive relationship between m and β_K was reported for the thin-film geometry of polystyrene [45]. The origin of the dynamical heterogeneity has two parts: One is an intrinsic heterogeneity related to the α process, even in the bulk, and the other is heterogeneity induced by the geometrical restriction in thin films. The value of β_K is determined by both factors in the case of thin polymer films, and accordingly, this leads to a different relationship between β_K and m.

Recently, the fragility index of freely standing PS films has been observed by dielectric relaxation spectroscopy and was found to decrease with decreasing film thickness down to the monomer limit [46]. The decrease in fragility index was attributed to an increase in the fraction of free surfaces in freely standing films. Comparing the present result with that of freely standing films, it should be noted that the increase in the fragility index for isothermal annealing of stacked thin polymer films might correspond to the increase in fragility index for the increase in film thickness in freely standing films. Therefore, the interface between stacked layers can play a crucial role similar to the free surface of freely standing films as far as the non-Arrhenius temperature dependence of the α-relaxation time, i.e., the fragility index, is concerned.

VI. CONCLUDING REMARKS

The glass transition behavior of stacked layers of thin films of polystyrene and poly(2-chlorostyrene) was investigated using differential scanning calorimetry and dielectric relaxation spectroscopy. The results obtained can be summarized as follows:

(1) Stacked thin films exhibit glass transition dynamics that are similar to those observed for single thin films. The glass transition temperature of as-stacked thin films is lower than that of the single thin supported films with the same thickness as that of a single layer in the stacked thin films, and is higher than that of freely standing films.

(2) Isothermal annealing can change the glass transition temperature and the dynamics of stacked thin films from thin-film-like dynamics to bulk-like dynamics.

(3) The characteristic time for evolution of the α dynamics for stacked thin films is very large compared with the reptation time of polymer chains.

(4) The relation between non-exponentiality and fragility for stacked thin films is different from that of conventional glassy systems.

In Sec. IV, the shift in the peak frequency of the dielectric loss due to the α process was discussed. However, in Fig. 2, an increase in the relaxation strength, i.e., the area below the α-relaxation peak, can also be observed with increase in the annealing time. The peak height in ε'' increases by 19.5% when the annealing time elapsed from 0 h to 173.4 h. The value of ε'' plotted in Fig. 2 was not corrected for any variation in film thickness due to isothermal annealing. The variation in film thickness was found to contribute to the apparent increase in ε'' by 6.3% from the analysis of the real part of electric capacitance at 273 K and 100 kHz for both $t_a = 0$ h and 173.4 h. Therefore, there should be an intrinsic increase in ε'' during the isothermal annealing process. In Ref. [47], it has been reported that the relaxation strength of the α process of the ultrathin films is smaller than that of the bulk. A possible origin of this increase in ε'' observed for the annealing of the stacked thin films may be associated with the reduction of the relaxation strength of the single ultrathin polymer films. The detailed investigation of variation of the dielectric relaxation strength for P2CS and PS is now still in progress in order to elucidate the origin of the increase with annealing time.

It was discussed in Sec. IV that there is a very slow change in the α dynamics in stacked thin films of P2CS. There may be several possibilities for this slow change. If heterogeneous diffusion in thin polymer layers is an essential process, then direct measurement of the diffusion constant of a tracer polymer chain in a thin layer of the stacked thin film is required. Recently, an alternative measurement of the diffusion constant of a polymer chain has been proposed

[33]. Such measurements could be applicable for the present case.

If the change in the quality of the contact surface is associated with the observed phenomena, similar measurements performed under external stress are required to elucidate the strong stress dependence of the time evolution of the α dynamics observed in stacked thin films.

Although there are many issues to be clarified, the present measurements provide clear evidence that a change in interfacial interaction is directly associated with the change in the glass transition dynamics for isothermal annealing processes.

ACKNOWLEDGMENTS

The authors would like to thank Professor T. Kanaya, Professor A. Toda, and Dr. T. Yamaguchi for useful discussions and suggestions. This work was supported by Grants-in-Aid for Scientific Research (B) (No. 21340121) and Exploratory Research (No. 23654154) from the Japan Society for the Promotion of Science, Scientific Research in the Priority Area "Soft Matter Physics" and "High-Tech Research Center" Project for Private Universities: matching funds subsidy from the Ministry of Education, Culture, Sports, Science, and Technology of Japan.

[1] K. L. Ngai, in *Physical Properties of Polymers*, edited by J. Mark *et al.*, Chap. 2 (Cambridge University Press, Cambridge, 2003).
[2] J. Keddie, R. A. L. Jones, and R. A. Cory, Europhys. Lett. **27**, 59 (1994).
[3] J. L. Keddie and R. A. L. Jones, Faraday Discuss. **98**, 219 (1994).
[4] J. Schüller, Yu. B. Mel'nichenko, R. Richert, and E. W. Fischer, Phys. Rev. Lett. **73**, 2224 (1994).
[5] G. B. DeMaggio, W. E. Frieze, D. W. Gidley, Ming Zhu, H. A. Hristov, and A. F. Yee, Phys. Rev. Lett. **78**, 1524 (1997).
[6] W. E. Wallace, J. H. van Zanten, and W. L. Wu, Phys. Rev. E **52**, R3329 (1995).
[7] B. Jerome and J. Commandeur, Nature (London) **386**, 589 (1997).
[8] M. Yu. Efremov, E. A. Olson, M. Zhang, Z. Zhang, and L. H. Allen, Phys. Rev. Lett. **91**, 085703 (2003).
[9] V. Lupascu, H. Huth, C. Schick, and M. Wübbenhorst, Thermochim. Acta **432**, 222 (2005).
[10] D. B. Hall, J. C. Hooker, and J. M. Torkelson, Macromolecules **30**, 667 (1997).
[11] K. Fukao and Y. Miyamoto, Europhys. Lett. **46**, 649 (1999).
[12] K. Fukao and Y. Miyamoto, Phys. Rev. E **61**, 1743 (2000).
[13] Y. Grohens, L. Hamon, G. Reiter, A. Soldera, and Y. Holl, Eur. Phys. J. E **8**, 217 (2002).
[14] J. S. Sharp and J. A. Forrest, Phys. Rev. E **67**, 031805 (2003).
[15] C. J. Ellison and J. M. Torkelson, Nature Mater. **2**, 695 (2003).
[16] C. B. Roth and J. R. Dutcher, Eur. Phys. J. E **12**, S103 (2003).
[17] C. J. Ellison, M. K. Mundra, and J. M. Torkelson, Macromolecules **38**, 1767 (2005).
[18] M. Arndt, R. Stannarius, H. Groothues, E. Hempel, and F. Kremer, Phys. Rev. Lett. **79**, 2077 (1997).
[19] L. Hartmann, W. Gorbatschow, J. Hauwende, and F. Kremer, Eur. Phys. J. E **8**, 145 (2002).
[20] H. Huth, A. A. Minakov, A. Serghei, F. Kremer, and C. Schick, Euro. Phys. J. Special Topics **141**, 153 (2007).
[21] M. Tress, M. Erber, E. U. Mapesa, H. Huth, J. Mller, A. Serghei, C. Schick, K.-J. Eichhorn, B. Voit, and F. Kremer, Macromolecules **43**, 9937 (2010).
[22] T. Kajiyama, K. Tanaka, I. Ohki, S-R. Ge, S. J. Yoon, and A. Takahara, Macromolecules **27**, 7932 (1994).
[23] M. Alcoutlabi and G. B. McKenna, J. Phys. Condens. Matter **17**, R461 (2005).
[24] P. K. Yung, G. B. McKenna, and S. L. Simon, J. Polym. Sci. Part B: Polym. Phys. **44**, 3518 (2006).
[25] P. K. Yung and S. L. Simon, J. Polym. Sci. Part B: Polym. Phys. **46**, 2741 (2008).
[26] K. Fukao, Y. Oda, K. Nakamura, and D. Tahara, Euro. Phys. J. Special Topics **189**, 165 (2010).
[27] G. Tsagaropoulos and A. Eisenberg, Macromolecules **28**, 6067 (1995).
[28] K. Tanaka, Y. Tateishi, Y. Okada, T. Nagamura, M. Doi, and H. Morita, J. Phys. Chem. B **113**, 4571 (2009).
[29] J. A. Forrest, K. Dalnoki-Veress, J. R. Stevens, and J. R. Dutcher, Phys. Rev. Lett. **77**, 2002 (1996).
[30] N. G. McCrum, B. E. Read, and G. Williams, *Anelastic and Dielectric Effects in Polymer Solids* (John Wiley & Sons, London, 1967), p. 414, Fig. 10.35.
[31] S. J. Whitlow and R. P. Wool, Macromolecules **24**, 5926 (1991).
[32] S. Napolitano and M. Wübbenhorst, Nature Commun. **2**, 260 (2011).
[33] S. Napolitano, C. Rotella, and M. Wübbenhorst, Macromol. Rapid Comm. **32**, 844 (2011).
[34] R. Inoue, K. Kawashima, K. Matsui, T. Kanaya, K. Nishida, G. Matsuba, and M. Hino, Phys. Rev. E **83**, 021801 (2011).
[35] F. B. Bowden and D. Tabor, *The Friction and Lubrication of Solids* (Clarendon, Oxford, 1954).
[36] J. H. Dieterich and G. Conrad, J. Geophys. Res. **89**, 4196 (1984).
[37] R. D. Priestley, L. J. Broadbelt, J. M. Torkelson, and K. Fukao, Phys. Rev. E **75**, 061806 (2007).
[38] S. Havriliak and S. Negami, Polymer **8**, 161 (1967).
[39] G. Williams and D. C. Watts, Trans. Faraday Soc. **66**, 80 (1970).
[40] F. Alvarez, A. Alegria, and J. Colmenero, Phys. Rev. B **44**, 7306 (1991).
[41] H. Vogel, Phys. Z. **22**, 645 (1921); G. S. Fulcher, J. Am. Chem. Soc. **8**, 339, 789 (1925).
[42] R. Böhmer and C. A. Angell, Phys. Rev. B **45**, 10091 (1992).
[43] R. Böhmer, K. L. Ngai, C. A. Angell, and D. J. Plazek, J. Chem. Phys. **99**, 4201 (1993).
[44] P. G. Debenedetti and F. H. Stillinger, Nature (London) **410**, 259 (2001).
[45] K. Fukao and Y. Miyamoto, Phys. Rev. E **64**, 011803 (2001).
[46] S. Napolitano and M. Wübbenhorst, Polymer **51**, 5309 (2010).
[47] K. Fukao, S. Uno, Y. Miyamoto, A. Hoshino, and H. Miyaji, Phys. Rev. E **64**, 051807 (2001).